and 90 non-Japanese individuals have been reported with this syndrome [6–9].

On the other hand, type 1 diabetes mellitus (DM) is a metabolic disorder characterized by diminished insulin production caused by the destruction of pancreatic β cells [10,11]. In most cases, an abnormal immunoresponse is involved in the pathogenesis of type 1 DM and autoimmune antibodies are often detectable. Recently, several congenital diseases were identified as being associated with the occurrence of DM [12], including Down's syndrome [13] and Wolframs syndrome [14]. In this report, we introduce a patient with Kabuki syndrome who developed type 1 DM and we discuss the possibility of an association between Kabuki syndrome and type 1 DM.

2. Case report

The patient was the second child of non-consanguineous Japanese parents, delivered at a birth weight of 2.7 kg following an uneventful 38-week pregnancy. Her parents and brothers were all healthy, of normal height and exhibited no anomalies. When she was 5 months of age, it was noted that the patient had both mental and growth retardation. In 1984 (age 15), she began regular menstruation. In 1987 (age 18), urinary glucose was 3+ and a 75-g oral glucose tolerance test (OGTT) revealed impaired glucose tolerance (IGT). In 1989 (age 20), the patient experienced a significant loss of weight (10 kg in 1 year) together with amenorrhea, but no symptoms of infection and was hospitalized for further examination. At that time, her height was 139 cm, her weight was 32 kg (BMI = 16.6 kg/m^2) and it was noted that she had arched eyebrows with sparse lateral halves, long palpebral fissures, eversion of the lower lateral eyelids, long eyelashes, large and prominent ears, a low posterior hair line (Fig. 1) and mild lumber scoliosis. Her fingers were stubby with clinodactyly of the bilateral fifth fingers (Fig. 2) and the second toes were bilaterally hypoplastic. Fingertip pads were found on all fingers. Her intelligence quotient was estimated to be 48. She had no pneumonia, otitis media or urinary tract infections.

Laboratory studies showed the patient's casual serum glucose to be 400 mg/dl, serum C-peptide immunoreactivity was 1.3 ng/ml, urinary C-peptide was 20 μg per day and she was positive for islet cell autoantibodies (ICA). As soon as type 1 DM was diagnosed, insulin therapy (28 U per day) was started. Additional analyses revealed mild anemia (Hb, 10.3 g/dl), moderate liver dysfunction (serum aspartate aminotransferase (AST), alanine aminotransferase (ALT), alkaline phosphatase (ALP) and γ-glutamyl transpeptidase (γ-GTP) were 37, 117, 237 and 62 IU/l, respectively), a somewhat low serum IgA level (57 g/dl) and that the patient was positive for anti-nucleic antibody (speckled pattern 40 times). An LH–RH test suggested slight hypothalamic pituitary dysfunction (maximum LH was 15 mIU/ml). Hormone replacement treatment, i.e. Holmstrom therapy (dydrogesterone, 10 mg per day for 7 days starting on day 21 of the menstrual cycle) was initiated and effective. Other laboratory data are shown in Tables 1–3. A liver biopsy was nearly normal. Roentgenograms showed mild lumbar scoliosis. Abdominal computed tomography showed a horseshoe kidney. Ultrasound cardiography showed no heart abnormalities and G-banding analysis of the karyotypes of cultured peripheral blood lymphocytes also showed no abnormalities.

Despite frequent infusions of rapid insulin combined with NPH insulin, the patient's diabetes has not been well controlled (HbA_{1c} was currently at ≈9%). At age 27, she contracted a common cold that resulted in her developing bronchitis. When admitted to the hospital because of drowsiness, she was diagnosed as having diabetic ketoacidosis based on the following parameters: serum glucose 600 mg/dl, urinary ketotic body 3+, pH 7.160, PO_2 135 mEq/l, PCO_2 9.2 mEq/l, HCO_3 3.3 mEq/l and O_2Sat 98%. Given hydration and intensive insulin therapy, her condition improved within a few days. In 1998, the patient was determined to be positive for anti-glutamic acid decarboxylase (GAD65) antibody (49,700 U/ml; normal range <1.4 by RIA) and her ability to secrete insulin has steadily declined by 2000, serum C-peptide was 0.1 ng/ml and urinary C-peptide was 0.2 μg per day. She experienced similar episodes of diabetic ketoacidosis induced by bron-

Fig. 1. The patient exhibited the typical facial abnormalities of Kabuki syndrome: arched eyebrows with sparse lateral halves, long palpebral fissures, eversion of the lower lateral eyelids, long eyelashes and large, prominent ears.

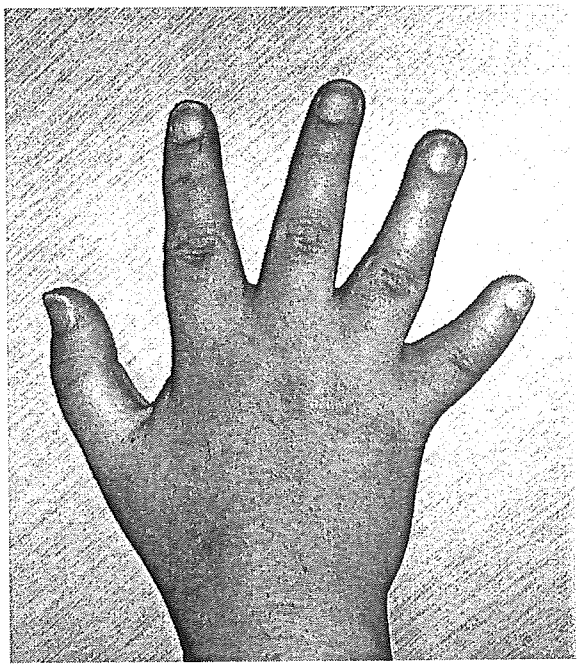

Fig. 2. Right hand of this patient shows the short, stubby, inwardly curved fifth fingers frequently seen in patients with Kabuki syndrome.

chitis at ages 29, 30 and 31 (in 1998, 1999 and 2000, respectively).

3. Discussion

Diabetes mellitus is a group of metabolic diseases characterized by hyperglycemia resulting from defects in insulin secretion, insulin action or both. The vast majority of diabetes cases fall into two broad etiopathogenetic categories termed 'type 1' and 'type 2' [12]. In type 1 DM, the cause is an absolute deficiency of insulin secretion, usually resulting from cell-mediated autoimmune destruction of the β-cells of the pancreas. This autoimmune response is often indicated by the presence of ICA, autoantibodies to insulin (IAAs) and/or autoantibodies to GAD65. In addition, this disease has strong human leukocyte antigen (HLA) associations, with linkage to specific HLA-DR/DQ alleles. Still, some forms of type 1 DM have unknown etiologies with no associations with HLAs, and in some cases, infection with certain viruses, including Coxsackie-virus B [15–18], cytomegalovirus [19–21], adenovirus [18,22]

Table 1
Clinical data at admission in 1989

CBC	
WBC	3800/μl
RBC	474×10^4/μl
Hb	10.3 g/dl
Ht	33.4%
Plt	22.9×10^4/μl
Biochemistry	
TP	6.5 g/dl
Alb	3.8 g/dl
T-Bil	0.3 g/dl
AST	37 IU/l
ALT	117 IU/l
LDH	119 IU/l
CPK	29 IU/l
ALP	237 IU/l
γ-GTP	62 IU/l
LAP	60 IU/l
ChE	538 IU/l
Amy	103 mg/dl
TTT	0.8 U
ZTT	2.2 U
BUN	16 mg/dl
Cre	0.4 mg/dl
UA	2.7 mg/dl
Na	140 mEq/l
K	3.5 mEq/l
Cl	100 mEq/l
Ca	8.3 mg/dl
P	3.0 mg/dl
T-Cho	100 mg/dl
TG	74 mg/dl
Glucose	237 mg/dl
HbA_{1c}	15.1%
Blood gas analysis (room air)	
pH	7.363
PO_2	106.2 mmHg
PCO_2	30.3 mmHg
HCO_3–	17.0 mmol/l
BE	−7.2
Urinalysis	
Gravity	1.030
pH	7.0
Protein	85 mg/day
Sugar	113.8 g/day
Ketone body	–
ESR	17 mm/h
CRP	0.3 mg/dl

Table 2
Immunological examination

Serum IgA	57 g/dl
IgG	1171 g/dl
IgM	296 g/dl
CH50	49 U/ml
C3	61 mg/dl
C4	28 mg/dl
Anti nucleic antibody	Speckled type; 40 times
Islet cell autoantibodies (ICA)	Positive
Anti dsDNA antibody	Negative
Anti ssDNA	Negative
Anti SS-A antibody	Negative
Anti SS-B antibody	Negative
Anti Scl 70 antibody	Negative
Rheumatoid factor	Negative
Anti cardiolipin antibody	Negative
Anti mitochondrial antibody	Negative
Anti TSH receptor antibody	Negative
Coombs tests	Negative
Anti HCV antibody	Negative
Anti HBs antigen	Negative
Anti Hepes Zoster virus antibody (CF)	Less than four times
Anti Cytomegalovirus antibody (CF)	Less than four times
Anti Rubella virus antibody (HI)	16 times
Anti Coxsackie-virus B 1-6 (CF)	All of them less than four times
VCA-IgG	160 times
VCA-IgM	Less than ten times
Anti early antigen-IgG	Less than ten times
Anti EBNA antibody	Less than ten times
HLA typing	A2, A26(10) B60(40), B62(15) CW3 DR4, DR12(5)

Table 3
Endocrinological examination

TSH	2.7 μU/ml
Free T4	0.9 ng/dl
Growth hormone	2.8 ng/ml
Cortisol	52 μg/dl
Somatomedin C	22 ng/ml
FSH	7.7 mIU/ml
LH	1.7 mIU/ml
PRL	2.0 ng/ml
Estradiol	0.8 pg/ml

and mumps [23,24], has been implicated in its pathogenesis.

On the other hand, a diagnosis of Kabuki syndrome is made on the basis of mental retardation, developmental delay and characteristic facial and skeletal abnormalities [3]. The incidence of Kabuki syndrome among Japanese newborns is estimated to be 1 in 32,000 and no consistent causal factors have yet been identified. With the exception of five families in which it runs as an autosomal dominant trait [25–28], the reported cases of Kabuki syndrome have been sporadic. Furthermore, although chromosomal abnormalities are reportedly associated with Kabuki syndrome in some cases [3–5], no such chromosomal abnormality was seen in our case.

As this is the first report, to our knowledge, of an association between Kabuki syndrome and type 1 DM, it is reasonable to consider this case to represent a chance association. In addition, the fact that this patient has HLA-DR4, one of the susceptible DR allele in Japanese type 1 DM, may support an occurrence of type 1 DM independent from that of Kabuki syndrome. On the other hand, if we assume that a common pathogenesis is present in the co-occurrence of type 1 DM and Kabuki syndrome, two possible mechanisms can be considered. The first involves the increased susceptibility to infection seen in Kabuki syndrome patients [3,29]. Indeed, recurrent otitis media and frequent upper respiratory infections are often reported in patients with Kabuki syndrome; in our case, prolonged bronchial infection preceded the patient's diabetic ketoacidosis on all occasions. It is unclear whether structural anomalies of organs or immune dysfunction is involved in the increased susceptibility to infection. On the other hand, as mentioned above, infection with some viruses can induce or at least trigger type 1 DM. Such viruses might therefore be the link between Kabuki syndrome and the occurrence of type 1 DM. However, our case had no apparent evidence of viral infections as a trigger of type 1 DM, which indicates lack of a viral infection-mediated association between these two diseases. Furthermore, since there is little evidence indicating that immunodeficient subjects tend to develop type 1 DM, this possibility may be rather unlikely.

Alternatively, we can speculate that selective IgA deficiency [30–32], one of the immunological manifestations of Kabuki syndrome [3], could be related to the occurrence of type 1 DM. Indeed, it has been reported that subjects with IgA deficiency have a significantly higher frequency of autoimmune diseases such as systemic lupus erythematosus (SLE), rheumatic arthritis and type 1 DM [33–39]. HLA-DQB1 alleles encoding non-Asp residues at position 57 are associated with susceptibility to both type 1 DM and selective IgA deficiency, providing a possible basis for increased co-occurrence of the two diseases [32,34,35,40–43]. Although DQB1 genotype in our patient has not been typed, her serum IgA was somewhat low. In this regard, IgA deficiency may be one of the factors connecting Kabuki syndrome and type 1 DM.

The second possibility involves autoimmune diseases themselves actually contributing to a link between Kabuki syndrome and type 1 DM. Certain autoimmune diseases, such as Hashimoto disease, a form of autoimmune thyroiditis [44], idiopathic thrombocytopenic purpura [45] and autoimmune hemolytic anemia [9], have been reported to be co-exist with Kabuki syndrome, though the frequency of autoimmune diseases being associated with Kabuki syndrome is not particularly high.

Taken these observations together, it is difficult to identify the background factor(s) possibly contributing to the association between Kabuki syndrome and type 1 DM and at present, we must consider our case as perhaps representing a chance association. However, we cannot rule out the possibility that type 1 DM is an autoimmune disease that tends to co-occur with Kabuki syndrome. Thus, we advocate further clinical investigations regarding the coexistence of autoimmune diseases, including type 1 DM, with Kabuki syndrome.

References

[1] N. Niikawa, N. Matsuura, Y. Fukushima, T. Ohsawa, T. Kajii, Kabuki make-up syndrome: a syndrome of mental

retardation, unusual facies, large and protruding ears, and postnatal growth deficiency, J. Pediatr. 99 (1981) 565–569.
[2] Y. Kuroki, Y. Suzuki, H. Chyo, A. Hata, I. Matsui, A new malformation syndrome of long palpebral fissures, large ears, depressed nasal tip, and skeletal anomalies associated with postnatal dwarfism and mental retardation, J. Pediatr. 99 (1981) 570–573.
[3] N. Niikawa, Y. Kuroki, T. Kajii, et al., Kabuki make-up (Niikawa-Kuroki) syndrome: a study of 62 patients, Am. J. Med. Genet. 31 (1988) 565–589.
[4] M.J. McGinniss, D.H. Brown, L.W. Burke, J.T. Mascarello, M.C. Jones, Ring chromosome X in a child with manifestations of Kabuki syndrome, Am. J. Med. Genet. 70 (1997) 37–42.
[5] J.P. Fryns, H. Van den Berghe, C. Schrander-Stumpel, Kabuki (Niikawa-Kuroki) syndrome and paracentric inversion of the short arm of chromosome 4, Am. J. Med. Genet. 53 (1994) 204–205.
[6] C. Schrander-Stumpel, P. Meinecke, G. Wilson, et al., The Kabuki (Niikawa-Kuroki) syndrome: further delineation of the phenotype in 29 non-Japanese patients, Eur. J. Pediatr. 153 (1994) 438–445.
[7] H. Ilyina, I. Lurie, I. Naumtchik, et al., Kabuki make-up (Niikawa-Kuroki) syndrome in the Byelorussian register of congenital malformations: ten new observations, Am. J. Med. Genet. 56 (1995) 127–131.
[8] E. Galan-Gomez, J.J. Cardesa-Garcia, F.M. Campo-Sampedro, C. Salamanca-Maesso, M.L. Martinez-Frias, J.L. Frias, Kabuki make-up (Niikawa-Kuroki) syndrome in five Spanish children, Am. J. Med. Genet. 59 (1995) 276–282.
[9] H. Kawame, M.C. Hannibal, L. Hudgins, R.A. Pagon, Phenotypic spectrum and management issues in Kabuki syndrome, J. Pediatr. 134 (1999) 480–485.
[10] G.S. Eisenbarth, Type I diabetes mellitus. A chronic autoimmune disease, New Engl. J. Med. 314 (1986) 1360–1368.
[11] J.F. Bach, Insulin-dependent diabetes mellitus as an autoimmune disease, Endocr. Rev. 15 (1994) 516–542.
[12] Expert Committee on the Diagnosis and Classification of Diabetes Mellitus, Report of the Expert Committee on the Diagnosis and Classification of Diabetes Mellitus, Diabetes Care 25 (2002) S5–S20.
[13] A.J. Anwar, J.D. Walker, B.M. Frier, Type 1 diabetes mellitus and Down's syndrome: prevalence, management and diabetic complications, Diabetic Med. 15 (1998) 160–163.
[14] T.G. Barrett, S.E. Bundey, Wolfram (DIDMOAD) syndrome, J. Med. Genet. 34 (1997) 838–841.
[15] J.W. Yoon, M. Austin, T. Onodera, A.L. Notkins, Isolation of a virus from the pancreas of a child with diabetic ketoacidosis, New Engl. J. Med. 300 (1979) 1173–1179.
[16] R. Gladisch, W. Hofmann, R. Waldherr, Myocarditis and insulitis following Coxsackie virus infection, Z. Kardiol. 65 (1976) 837–849.
[17] A.B. Jenson, H.S. Rosenberg, A.L. Notkins, Pancreatic islet-cell damage in children with fatal viral infections, Lancet 2 (1980) 354–358.
[18] D.B. Jones, I. Crosby, Proliferative lymphocyte responses to virus antigens homologous to GAD65 in IDDM, Diabetologia 39 (1996) 1318–1324.
[19] K.P. Ward, W.H. Galloway, I.A. Auchterlonie, Congenital cytomegalovirus infection and diabetes, Lancet 1 (1979) 497.
[20] C.Y. Pak, H.M. Eun, R.G. McArthur, J.W. Yoon, Association of cytomegalovirus infection with autoimmune type 1 diabetes, Lancet 2 (1988) 1–4.
[21] N. Yasumoto, M. Hara, Y. Kitamoto, M. Nakayama, T. Sato, Cytomegalovirus infection associated with acute pancreatitis, rhabdomyolysis and renal failure, Intern. Med. 31 (1992) 426–430.
[22] H.M. Surcel, J. Ilonen, M.L. Kaar, H. Hyoty, P. Leinikki, Infection by multiple viruses and lymphocyte abnormalities at the diagnosis of diabetes, Acta Paediatr. Scand. 77 (1988) 471–474.
[23] K. Helmke, A. Otten, W. Willems, Islet cell antibodies in children with mumps infection, Lancet 2 (1980) 211–212.
[24] D.R. Gamble, Relation of antecedent illness to development of diabetes in children, Br. Med. J. 281 (1980) 99–101.
[25] F. Halal, R. Gledhill, A. Dudkiewicz, Autosomal dominant inheritance of the Kabuki make-up (Niikawa-Kuroki) syndrome, Am. J. Med. Genet. 33 (1989) 376–381.
[26] O. Kobayashi, N. Sakuragawa, Inheritance in Kabuki make-up (Niikawa-Kuroki) syndrome, Am. J. Med. Genet. 61 (1996) 92–93.
[27] M. Silengo, M. Lerone, M. Seri, G. Romeo, Inheritance of Niikawa-Kuroki (Kabuki makeup) syndrome, Am. J. Med. Genet. 66 (1996) 368.
[28] M. Tsukahara, Y. Kuroki, K. Imaizumi, Y. Miyazawa, K. Matsuo, Dominant inheritance of Kabuki make-up syndrome, Am. J. Med. Genet. 73 (1997) 19–23.
[29] K.H. Chrzanowska, M. Krajewska-Walasek, J. Kus, et al., Kabuki (Niikawa-Kuroki) syndrome associated with immunodeficiency, Clin. Genet. 53 (1998) 308–312.
[30] A.J. Burks, R.W. Steele, Selective IgA deficiency, Ann. Allergy 57 (1986) 3–13.
[31] M. Fiore, C. Pera, L. Delfino, I. Scotese, G.B. Ferrara, C. Pignata, DNA typing of DQ and DR alleles in IgA-deficient subjects, Eur. J. Immunogenet. 22 (1995) 403–411.
[32] O. Olerup, C.I. Smith, L. Hammarstrom, Different amino acids at position 57 of the HLA-DQ beta chain associated with susceptibility and resistance to IgA deficiency, Nature 347 (1990) 289–290.
[33] R.S. Liblau, S. Caillat-Zucman, A.M. Fischer, J.F. Bach, C. Boitard, The prevalence of selective IgA deficiency in type 1 diabetes mellitus, APMIS 100 (1992) 709–712.
[34] W.J. Smith, B.S. Rabin, A. Huellmantel, D.H. Van Thiel, A. Drash, Immunopathology of juvenile-onset diabetes mellitus. I. IgA deficiency and juvenile diabetes, Diabetes 27 (1978) 1092–1097.

[35] S. Hoddinott, J. Dornan, J.C. Bear, N.R. Farid, Immunoglobulin levels, immunodeficiency and HLA in type 1 (insulin-dependent) diabetes mellitus, Diabetologia 23 (1982) 326–329.
[36] M. Ambrus, E. Hernadi, G. Bajtai, Prevalence of HLA-A1 and HLA-B8 antigens in selective IgA deficiency, Clin. Immunol. Immunopathol. 7 (1977) 311–314.
[37] F. Perez-Jimenez, P.B. Lopez, E.P. Tallo, J.R. Guzman, J.S. Molina, J.A. Pereperez, Selective IgA deficiency and the HLA-B8 antigen. Report of two cases with familial data, Arch. Intern. Med. 141 (1981) 509–510.
[38] D.H. Van Thiel, W.I. Smith, Jr, B.S. Rabin, S.E. Fisher, R. Lester, A syndrome of immunoglobulin A deficiency, diabetes mellitus, malabsorption, a common HLA haplotype. Immunologic and genetic studies of forty-three family members, Ann. Intern. Med. 86 (1977) 10–19.
[39] G.A. Hagen, R.M. Bolman, III, J.P. Frank, Atypical adrenal insufficiency with failure of the pituitary feedback receptor. A case with associated diabetes mellitus and selective IgA deficiency with steatorrhea, Am. J. Med. 59 (1975) 882–888.
[40] J.A. Todd, J.I. Bell, H.O. McDevitt, HLA-DQ beta gene contributes to susceptibility and resistance to insulin-dependent diabetes mellitus, Nature 329 (1987) 599–604.
[41] J.A. Todd, Genetic control of autoimmunity in type 1 diabetes, Immunol. Today 11 (1990) 122–129.
[42] G.T. Horn, T.L. Bugawan, C.M. Long, H.A. Erlich, Allelic sequence variation of the HLA-DQ loci: relationship to serology and to insulin-dependent diabetes susceptibility, Proc. Natl. Acad. Sci. USA 85 (1988) 6012–6016.
[43] K.S. Ronningen, T. Iwe, T.S. Halstensen, A. Spurkland, E. Thorsby, The amino acid at position 57 of the HLA-DQ beta chain and susceptibility to develop insulin-dependent diabetes mellitus, Hum. Immunol. 26 (1989) 215–225.
[44] A. Ewart-Toland, G.M. Enns, V.A. Cox, G.C. Mohan, P. Rosenthal, M. Golabi, Severe congenital anomalies requiring transplantation in children with Kabuki syndrome, Am. J. Med. Genet. 80 (1998) 362–367.
[45] T. Watanabe, M. Miyakawa, M. Satoh, T. Abe, Y. Oda, Kabuki make-up syndrome associated with chronic idiopathic thrombocytopenic purpura, Acta Paediatr. Jpn. 36 (1994) 727–729.

Histochem Cell Biol (2003) 119:247–256
DOI 10.1007/s00418-003-0495-6

ORIGINAL PAPER

Kim Cryns · Sofie Thys · Lut Van Laer · Yoshitomo Oka · Markus Pfister · Luc Van Nassauw · Richard J. H. Smith · Jean-Pierre Timmermans · Guy Van Camp

The *WFS1* gene, responsible for low frequency sensorineural hearing loss and Wolfram syndrome, is expressed in a variety of inner ear cells

Accepted: 19 December 2002 / Published online: 19 February 2003

Abstract Heterozygous mutations in the *WFS1* gene are responsible for autosomal dominant low frequency hearing loss at the *DFNA6/14* locus, while homozygous or compound heterozygous mutations underlie Wolfram syndrome. In this study we examine expression of wolframin, the WFS1-gene product, in mouse inner ear at different developmental stages using immunohistochemistry and in situ hybridization. Both techniques showed compatible results and indicated a clear expression in different cell types of the inner ear. Although there were observable developmental differences, no differences in staining pattern or gradients of expression were observed between the basal and apical parts of the cochlea. Double immunostaining with an endoplasmic reticulum marker confirmed that wolframin localizes to this organelle. A remarkable similarity was observed between cells expressing wolframin and the presence of canalicular reticulum, a specialized form of endoplasmic reticulum. The canalicular reticulum is believed to be involved in the transcellular movements of ions, an important process in the physiology of the inner ear. Although there is nothing currently known about the function of wolframin, our results suggest that it may play a role in inner ear ion homeostasis as maintained by the canalicular reticulum.

Keywords *WFS1* · Inner ear · Immunohistochemistry · In situ hybridization · Canalicular reticulum

K. Cryns and S. Thys contributed equally

K. Cryns · S. Thys · L. Van Laer · G. Van Camp (✉)
Department of Medical Genetics,
University of Antwerp, Universiteitsplein 1,
2610 Antwerp, Belgium
e-mail: gvcamp@uia.ua.ac.be
Tel.: +32-3-8202585
Fax: +32-3-8202566

Y. Oka
Division of Molecular Metabolism and Diabetes,
Department of Internal Medicine,
Tohoku University Graduate School of Medicine,
980-8575 Seiryo-machi, Sendai, Japan

M. Pfister
Department of Otolaryngology,
University of Tübingen,
Elfriede-Aulhornstrasse 5, 72076 Tübingen, Germany

L. Van Nassauw · J.-P. Timmermans
Laboratory of Cell Biology and Histology,
University of Antwerp,
Groenenborgerlaan 171, 2020 Antwerp, Belgium

R. J. H. Smith
Molecular Otolaryngology Research Laboratories,
University of Iowa,
Iowa City, Iowa, 52242 USA

Introduction

Hearing loss is the most frequent sensory defect in humans and genes play an important role in its etiology. Over the past decade, tremendous progress has been made in the localization and identification of genes responsible for hereditary hearing impairment (HI). Of the currently mapped 41 chromosomal loci associated with autosomal dominant hearing loss (Van Camp and Smith 2002) two loci segregate low frequency sensorineural HI (*DFNA1* and *DFNA6/14*), suggesting that this form of hearing loss is less heterogeneous than either mid- or high frequency sensorineural HI. The gene for low frequency HI at the *DFNA1* locus is *DIAPH1*, the homologue of *Drosophila diaphanous* (Lynch et al. 1997). Recently, Bespalova et al. (2001) and Young et al. (2001) found the gene for the second locus (*DFNA6/14*). In total, these two groups found five different heterozygous mutations in the *WFS1* gene in seven *DFNA6/14* families. Cryns et al. (2002) added five additional *WFS1* mutations to this list in their study of four families and one isolated patient, all selected for mutation screening on the basis of their audioprofile.

Recessive mutations in the *WFS1* gene also cause Wolfram syndrome, known by the acronym DIDMOAD to reflect the syndrome phenotype of diabetes insipidus, diabetes mellitus, optic atrophy, and deafness (Inoue et al. 1998; Strom et al. 1998). In contrast to the low frequency

HI of *DFNA6/14* patients, the hearing loss associated with Wolfram syndrome mainly affects the high frequencies (Cremers et al. 1977; Higashi 1991).

The *WFS1* gene encodes an 890 amino acid protein (wolframin) that is predicted to have nine helical transmembrane segments (Strom et al. 1998) and probably represents a member of a novel gene family since no related proteins are listed in public databases. Biochemical studies indicate that wolframin may be an integral endoglycosidase H-sensitive membrane glycoprotein predominantly localized in the endoplasmic reticulum (ER; Takeda et al. 2001).

Because nothing is known about its function, it is difficult to determine the role of wolframin in the biology of hearing. As an important first step in elucidating this role, we sought to determinate the inner ear expression pattern of *WFS1* using complementary techniques [immunohistochemistry (IHC) and in situ hybridization (ISH)] at different developmental stages of murine inner ear development.

Materials and methods

Animals

Swiss mice of both sexes and from different stages of postnatal development were used: postnatal day 1 (PD1; n=4), 7 (PD7; n=3), 14 (PD14; n=6), and 35 (PD35; n=4). All animals had free access to water and complete rodent diet and were kept in a 12-h/12-h light/dark cycle. All experimental procedures were approved by the ethics committee of the University of Antwerp. Japanese White rabbits were used for antibody production and treated under the approval of the ethics committee of the Tohoku University Graduate School of Medicine.

Tissue preparation

Animals were killed by an intraperitoneally administered overdose of Nembutal (Sanofi, Brussels, Belgium). They were transcardially perfused with a Krebs solution (117 mM NaCl, 5 mM KCl, 2.5 mM $CaCl_2.2H_2O$, 1.2 mM $MgSO_4.7H_2O$, 1.2 mM $NaH_2PO_4.2H_2O$, 25 mM $NaHCO_3$, 10 mM glucose) containing 0.25% (v/v) heparin, followed by 4% paraformaldehyde in a 0.1 M phosphate buffer (pH 7.0). In PD14 and PD35 mice, the fixative was injected through the tympanic membrane prior to transcardial perfusion. Immediately after perfusion the mice were decapitated. Temporal bones were removed and postfixed for 4 h at 4°C when used for IHC or for 1 h at room temperature when used for ISH. For ISH all solutions were made with autoclaved diethylpyrocarbonate-treated bidistilled water (DEPC-H_2O). During postfixation, inner ears were dissected out of the temporal bones. Next, the inner ears were rinsed overnight in 0.01 M phosphate-buffered saline (PBS; pH 7.4). Inner ears from animals older than 6 days were decalcified for 1–3 weeks in PBS, containing 5% ethylenediaminetetraacetic acid (EDTA). The solution was renewed every 2–3 days. After rinsing in PBS, inner ears were paraffin-embedded and midmodiolar sections (5 μm) were mounted on polylysine-coated or silanized glasses for IHC and ISH, respectively.

Primary antibodies

A cDNA fragment encoding the N-terminal 290 amino acids of mouse WFS1 (mWFS1) was cloned into the pGEX-6P-1 plasmid (Amersham Bioscience, Tokyo, Japan) to produce chimeric proteins consisting of the N-terminal sequence of mWFS1 and the C-terminal glutathione *S*-transferase (GST) protein, termed WFS1n-GST. The cDNA encoding the N-terminal 179 amino acids of mWFS1 was also cloned into the pMAL-c2 plasmid (New England Biolaboratories, Mass., USA) to produce a fusion protein consisting of the N-terminal sequence of mWFS1 and maltose-binding protein (MBP), termed WFS1n-MBP. The WFS1n-GST and WFS1n-MBP fusion proteins were expressed in *Escherichia coli* (JM109 strain) and induced by 1 mM IPTG (isopropyl-thiogalactopyranoside). Bacterial lysates were mixed with glutathione Sepharose 4B (Amersham Bioscience, Tokyo, Japan) and amylose resin (New England Biolaboratories) for purification of WFS1n-GST and WFS1n-MPB, respectively. The bound WFS1n-GST fusion protein was eluted from glutathione Sepharose 4B by addition of 10 mM reduced glutathione solution. The eluted WFS1n-GST fusion protein was used for immunizing Japanese White rabbits. Rabbit antisera were collected and affinity purified using WFS1n-MBP bound to the amylose resin.

As a marker for ER, a commercially available affinity-purified chicken antibody (ABR Affinity Bioreagents, Golden, Colo., USA) was used, raised against a synthetic peptide corresponding to amino acid residues 24–43 from mouse calreticulin. Calreticulin is a major calcium-binding protein found in the lumen of the ER (Michalak et al. 1992; Nash et al. 1994)

Immunohistochemistry

All steps were performed at room temperature unless indicated otherwise. Paraffin sections were dewaxed in xylol and rehydrated in decreasing concentrations of ethanol. Subsequently, sections were rinsed in PBS and non-specific binding was blocked by immersion for 30 min in PBS containing 10% normal goat serum (Dako, Glostrup, Denmark), 0.05% thimerosal, 5% bovine serum albumin (BSA) and 0.3% Triton X-100. Next, sections were incubated overnight at 4°C with primary rabbit anti-WFS1 antibody, diluted 1:1,000 in PBS containing 0.3% Triton X-100 (tx-PBS). After rinsing in PBS, biotinylated Fab fragments of goat anti-rabbit immunoglobulin (Ig) G (Rockland, Gilbertsville, Pa., USA) diluted 1:3,000 in tx-PBS, were applied for 2 h. After washing in PBS, sections were immersed for 2 h in Cy3-conjugated streptavidin (Jackson Immunoresearch Laboratories, West Grove, Pa., USA), diluted 1:5,000 in PBS containing 0.001% BSA and 0.05% thimerosal. After a final rinse in PBS, sections were mounted in Citifluor (Ted Pella, Redding, Calif., USA) and studied with fluorescence and confocal microscopy.

To investigate the presence of WFS1 protein in the ER of the cells of the inner ear, we performed a sequential double immunolabeling using anti-WFS1 and the ER marker anti-calreticulin. WSF1 was visualized as described above. Subsequently, the sections were thoroughly rinsed in PBS and incubated overnight at 4°C with a 1:100 dilution of the chicken anti-calreticulin in tx-PBS. After rinsing in PBS, a fluorescein (FITC)-conjugated donkey anti-chicken IgG (Jackson Immunoresearch Laboratories), diluted 1:100 in tx-PBS, was applied for 2 h. After a final rinse in PBS, sections were mounted in Citifluor and evaluated using fluorescence and confocal microscopy.

Negative controls were treated as above, but either one of the primary antibodies was omitted or preimmune serum, diluted to the same extent, was used instead of the primary antibody. Preadsorption of the WFS1 antibody with the WFS1n-GST chimeric protein also was performed. For the double labeling, we checked crossreactivity of the secondary antibodies by staining with primary antibodies and the non-corresponding secondary antibodies.

Probe synthesis for ISH

A 981-bp mouse *WFS1* fragment (nucleotides 929–1909; Genbank accession number NM_011716) was cloned into a pCR4-TOPO cloning vector (Invitrogen, Carlsbad, Calif., USA) according to the manufacturer's instructions. Plasmids were linearized with *Not*I or

*Spe*I and digests were purified using the Concert Rapid PCR Purification system (Life Technologies, Karlsruhe, Germany). Digoxigenin (DIG)-labeled antisense and sense riboprobes were generated with T3 or T7 polymerase using Riboprobe In Vitro Transcription Systems (Promega, Madison, Wis., USA) and DIG-11-UTP (Roche Diagnostics, Brussels, Belgium). The transcription reaction mixture contained transcription buffer, 10 mM dithiothreitol (DTT), 40 U RNase inhibitor, 1 mM ATP, GTP, and CTP, respectively, 0.65 mM UTP, 0.35 mM DIG-11-UTP, 1 µg linearized plasmid, and 40 U polymerase in a final reaction volume of 25 µl. The reaction was incubated for 1 h at 37°C and yeast tRNA (final concentration: 100 ng/µl) and 7.3 mM DTT were added to the reaction mixture. The solution was phenol-chloroform extracted and riboprobes were precipitated with 1/5 vol 10 M ammonium acetate and 3 vol ethanol. After centrifugation, pellets were dried and dissolved in 10 mM DTT. To allow better diffusion of the riboprobe into the tissue, alkaline hydrolysis of the probe was performed by adding 1/10 vol hydrolysis buffer (400 mM $NaHCO_3$, 600 mM Na_2CO_3, pH 10.2) followed by incubation at 60°C for 51 min. Hydrolysis was stopped by placing the probe on ice and by adding an equal volume hydrolysis-neutralization buffer (200 mM sodium acetate, 1% acetic acid, 10 mM DTT, pH 6). Subsequently, the probe was ethanol precipitated and pellets were dissolved in 20 µl DEPC-H_2O. Probe concentrations were determined using the DIG Nonradioactive Nucleic Acid Labeling and Detection system (Roche Diagnostics) following the manufacturer's protocol.

In situ hybridization

All steps were performed at room temperature unless indicated otherwise and all solutions were made with DEPC-H_2O. Freshly prepared paraffin sections were dewaxed in xylene and rehydrated in decreasing concentrations of ethanol to DEPC-H_2O and rinsed in PBS. After equilibration for 10 min at 37°C in a 0.1 M TRIS-HCl buffer (pH 8.0) containing 50 mM EDTA, sections were treated for 30 min at 37°C with 1 µg/ml proteinase K in the same buffer. After rinsing with PBS containing 0.2% glycine, sections were treated for 60 s at 4°C with an aquatic solution of 20% acetic acid, postfixed for 20 min at 4°C with PBS containing 0.4% paraformaldehyde, and acetylated for 10 min in a 0.1 M triethanolamine buffer (pH 8.0) containing 0.25% acetic anhydride. The hybridization solution contained 0.01 M TRIS-HCl buffer (pH 6.8), 0.3 M NaCl, 5 mM EDTA, 50% formamide, 10% dextran sulfate, 0.5xDenhardt's solution (Sigma, St. Louis, Mo., USA) and 1 µg/ml yeast tRNA (Roche Diagnostics). After prehybridization for 1 h at 60°C in hybridization solution without dextran sulfate, hybridization was performed overnight at 60°C with the species-specific DIG-labeled antisense riboprobe at a final concentration of 500 ng/ml. Following hybridization, sections were briefly washed in saline sodium citrate buffer (SSC) and then posthybridized for 2×15 min at 60°C in 50% formamide diluted in 2xSSC, followed by an incubation for 2×15 min at 60°C in 0.1xSSC. After rinsing with a TBS wash buffer (150 mM NaCl, 100 mM TRIS, pH 7.5, 0.05% Triton X-100) and blocking with TBS wash buffer containing a 0.5% blocking reagent (Roche Diagnostics), sections were incubated for 1 h with alkaline phosphatase-conjugated Fab fragments of a sheep anti-DIG antibody (Roche Diagnostics), diluted 1:750 in TRIS buffer (100 mM TRIS-HCl, 150 mM NaCl, pH 7.5) containing 5% normal sheep serum (Jackson Immunoresearch Laboratories). Signals were visualized by incubation for 3 h at 37°C with NBT/BCIP substrate (Dako). The reaction was stopped with TE buffer (10 mM TRIS, 1 mM EDTA, pH 8.0) and non-specific labeling was removed by incubation in 95% ethanol for 1 h. Sections were rinsed in bidistilled water and mounted in Aquamount (BDH Laboratory Supplies, Poole, UK).

Three types of negative controls were used: the omission of probe, the use of sense instead of antisense riboprobe (also at a final concentration of 500 ng/ml), and RNase treatment of the sections prior to hybridization. RNase treatment was performed for 30 min at 37°C in a solution containing 100 µg/ml RNase (Roche Diagnostics), 1 mM EDTA (pH 8), 10 mM TRIS (pH 8), and 5 M NaCl.

Northern blot analysis

The mouse *WFS1* cDNA probe (100 ng) was labeled with α-^{32}P dATP (3,000 Ci/mmol; ICN Pharmaceuticals, Costa Mesa, Calif., USA) and α-^{32}P (3,000 Ci/mmol; ICN Pharmaceuticals) using random priming according to standard procedures. Hybridization of the probe to a mouse MTN blot (BD Clontech Laboratories, Palo Alto, Calif., USA) was performed according to the manufacturer's instructions, except for the last wash step, which was omitted. The blot was exposed overnight to X-ray film at −80°C.

Results

WFS1 antibody

An antibody was raised against a 290 amino acid N-terminal fragment of mouse WFS1 and purified as described in Materials and methods. The antibody recognized a 100-kDa band, which corresponds to the apparent molecular mass of WFS1 protein, on immunoblotting of cell lysate of COS-7 cells transfected with the pcDNA3 (Invitrogen, Tokyo, Japan) containing mWFS1 cDNA (data not shown). Furthermore, this band was not observed when the antibody was preincubated with WFS1n-GST fusion protein (data not shown). These results indicate that the antibody specifically recognizes WFS1 protein.

Immunohistochemistry

We compared wolframin expression during postnatal development of the mouse inner ear at days 1, 7, 14, and 35 (mature inner ear), using an affinity-purified rabbit anti-WFS1 antibody. Negative controls showed no positive staining.

An overview of the distribution of wolframin in mouse inner ear is given in Table 1 and Figs. 1, 2, and 3. In 1-day-old mice, strong immunoreactivity was present in neurons of the spiral ganglion (Fig. 1a, b), Deiters' cells, inner hair cells (Fig. 1a) as well as in vestibular hair cells (Fig. 1d). Wolframin labeling in these regions was shown to persist at later stages of development and in mature inner ear. Moderate to intense staining of the outer hair cells (OHCs) was seen at PD1 (Fig. 1a), but expression in OHCs was lower in PD7 (Fig. 1e) and PD14 mice (Fig. 2a), and mostly absent in the mature inner ear (Fig. 3a).

External sulcus cells showed labeling at all developmental stages, with the most prominent staining observed at PD1 (Fig. 1a) and PD35 (Fig. 3b). Inner sulcus cells displayed strong expression in newborn mice (Fig. 1a), which gradually decreased during development and was almost completely absent in the mature stage. Strong immunostaining was also observed in marginal cells of the stria vascularis at PD1 (Fig. 1c). At later stages,

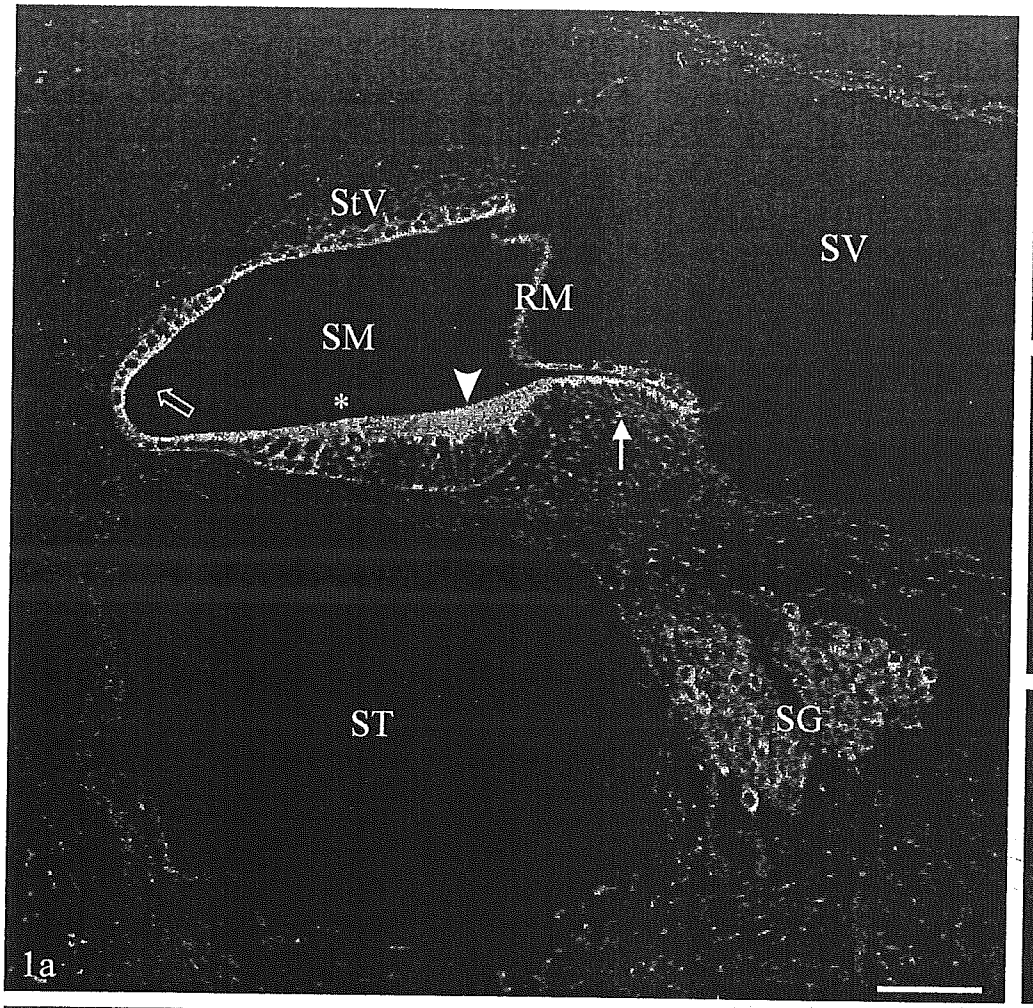
StV
SV
RM
SM
*
ST
SG
1a

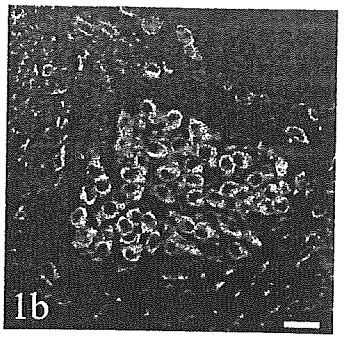
1b

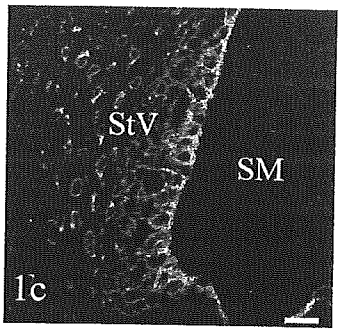
StV
SM
1c

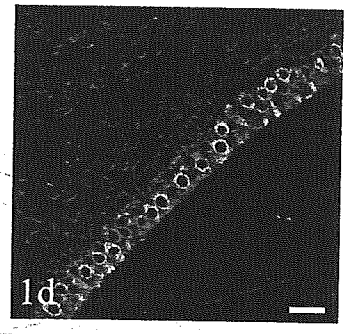
1d

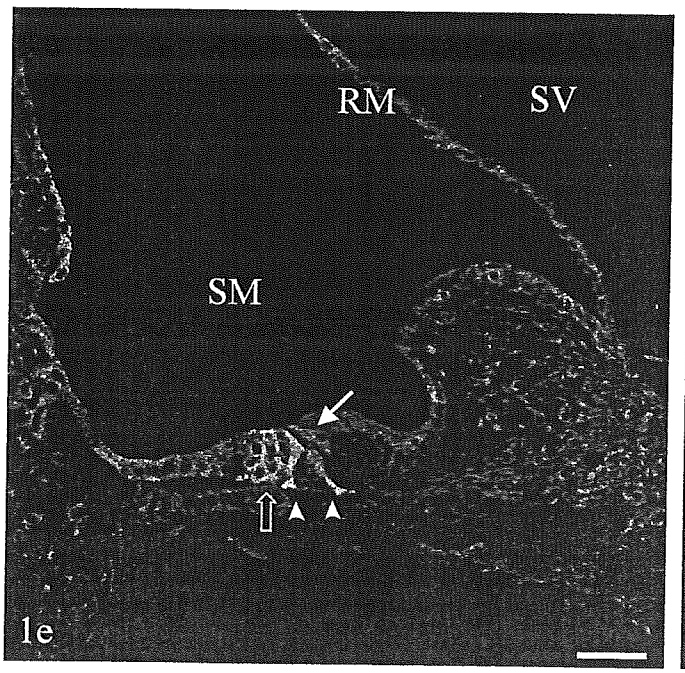
RM
SV
SM
1e

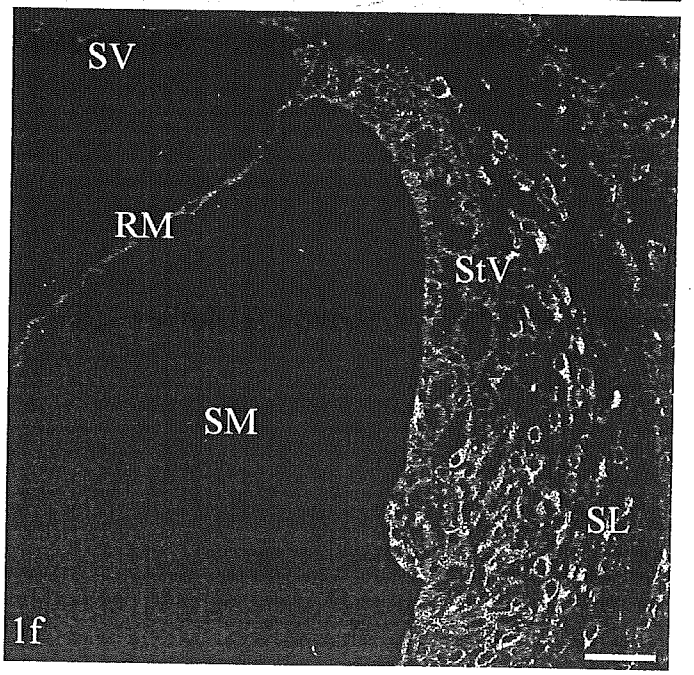
SV
RM
StV
SM
SL
1f

Table 1 Expression pattern of wolframin in mouse inner ear at postnatal day (*PD*) 1, 7, 14, and 35. The presence of canalicular reticulum, a specialized form of ER, is also indicated. – No wolframin expression can be detected, ± wolframin expression is weak or absent in some sections, + wolframin expression is present, ++ wolframin is strongly expressed, +/++ wolframin expression is present or strong depending on the sections

Inner ear structure	PD1	PD7	PD14	PD35	Canalicular reticulum[a]
Vestibular hair cells	++	++	++	++	Present (Cunningham et al. 2000)
Spiral ganglion	++	++	++	++	
Deiters' cells	++	++	++	++	Present (Harada et al. 1987)
Inner hair cells	++	+	++	++	Present (Spicer et al. 1999)
Outer hair cells	+/++	+	+	±	Present (Spicer et al. 1998)
External sulcus cells	++	+	+	+/++	Present (Spicer and Schulte 1997)
Inner sulcus cells	++	+	±	±	
Marginal cells of stria	++	±	+	–	Present (Forge 1982)
Intermediate cells of stria	–	–	–	–	
Basal cells of stria	–	–	–	–	
Hensen cells	++	±	+/++	+/++	Present (Harada et al. 1987)
Claudius cells	++	+	+	+/++	Present (poorly developed) (Harada et al. 1987)
Interdental cells	++	+	–	+	Present (Spicer et al. 2000)
Pillar cells	±	++	+/++	–	Present (Harada et al. 1987; Spicer et al. 2000)
Reissner's membrane	+	+	+	+	Present (Qvortrup and Rostgaard 1990)
Tympanic border cells	–	–	+	–	
Spiral ligament	–	+	–	+	Present in type I, II, IV, VI fibrocytes (Spicer and Schulte 1997)

[a] As far as we know, the presence of canalicular reticulum in mouse inner ear has not been studied yet. Therefore the references represent studies in other species (gerbil and guinea pig)

although wolframin labeling of the stria was reduced in comparison with PD1, at PD14 moderate staining still could be observed (Fig. 2c). However, in the fully developed inner ear, we did not observe any staining of the marginal cells. In none of the developmental stages we studied was wolframin immunostaining present in the intermediate or basal cells of the stria.

At all stages, immunoreaction, ranging from intermediate to strong, was observed in Hensen cells and Claudius cells (Figs. 1a, e, 2a, b, 3a). Wolframin was abundantly expressed in interdental cells at PD1 (Fig. 1a) but was completely absent in PD14 mice (Fig. 2a). At PD7 (Fig. 1e) and PD35 (Fig. 3c), the labeling was intermediate. High immunoreactivity was detected in pillar cells at PD7 (Fig. 1e) and moderate to high at PD14 (Fig. 2a, b); only a weak pillar cell signal was observed at PD1 (Fig. 1a) and no staining occurred in the mature stage (Fig. 3a).

Moderate staining of the Reissner's membrane was present at all stages, whereas no or very low wolframin protein levels were detectable at the spiral ligament, except at PD7 and PD35. At the latter stages, moderate immunoreactivity was observed in the spiral ligament (Figs. 1f, 3d). Labeling in the tympanic border cells was observed only at PD14 (Fig. 2a, b). In none of the developmental stages studied were differences in staining patterns or gradients of staining observed between basal and apical parts of the cochlea, based on comparison in midmodiolar sections.

Immunostaining of wolframin in cochlear cells suggested a netlike pattern consistent with localization of wolframin in the ER, as reported by Takeda et al. (2001) in cultured cells. To confirm this, we performed colocalization experiments with calreticulin, an ER-specific marker. Although an overlap between both signals was observed suggesting that wolframin colocalizes with calreticulin (Figs. 4, 5), expression of calreticulin was not equally intense in all cell types of the inner ear. For example, in Hensen cells calreticulin expression was very strong (Fig. 4b), while in other cells, expression was very low.

Fig. 1 Overview of wolframin immunoreactivity in paraffin sections of postnatal day (PD)1 (**a–d**) and PD7 (**e, f**) mouse inner ear. *Scale bar* 50 µm. **a** Cells lining the scala media (*SM*) and showing strong immunostaining are interdental cells (*thin arrow*), inner sulcus cells (*arrowhead*), Kollikers' organ (*asterisk*; inner hair cell, outer hair cells, Deiters' cells, Hensen cells, Claudius' cells), external sulcus cells (*open arrow*), and the marginal cells of the stria vascularis (*StV*). Furthermore, a strong immunoreaction was observed in the spiral ganglion (*SG*), whereas Reissner's membrane (*RM*) shows a moderate expression of wolframin. **b** Intense immunostaining of the spiral ganglion. **c** Marginal cells of the stria vascularis (*StV*), bordering the scala media (*SM*), show positive staining, while intermediate and basal cells do not. **d** Vestibular hair cells showing strong immunoreactivity. **e** Immunostaining is strong in pillar cells (*arrowheads*) and Deiters' cells (*open arrow*) and moderate to weak in interdental cells, inner sulcus cells, inner hair cell (*thin arrow*), outer hair cells, Claudius' cells, external sulcus cells, and Reissner's membrane (*RM*). **f** Positive reaction in fibrocytes of the spiral ligament (*SL*). *ST* Scala tympani, *SV* scala vestibuli

In situ hybridization

In situ hybridization was performed in order to confirm our results obtained by IHC. A species-specific probe was generated by cloning a 981-bp mouse *WFS1* fragment. A mouse multiple tissue northern blot was hybridized with this cloned fragment to determine its specificity and, in agreement with previous findings (Inoue et al. 1998;

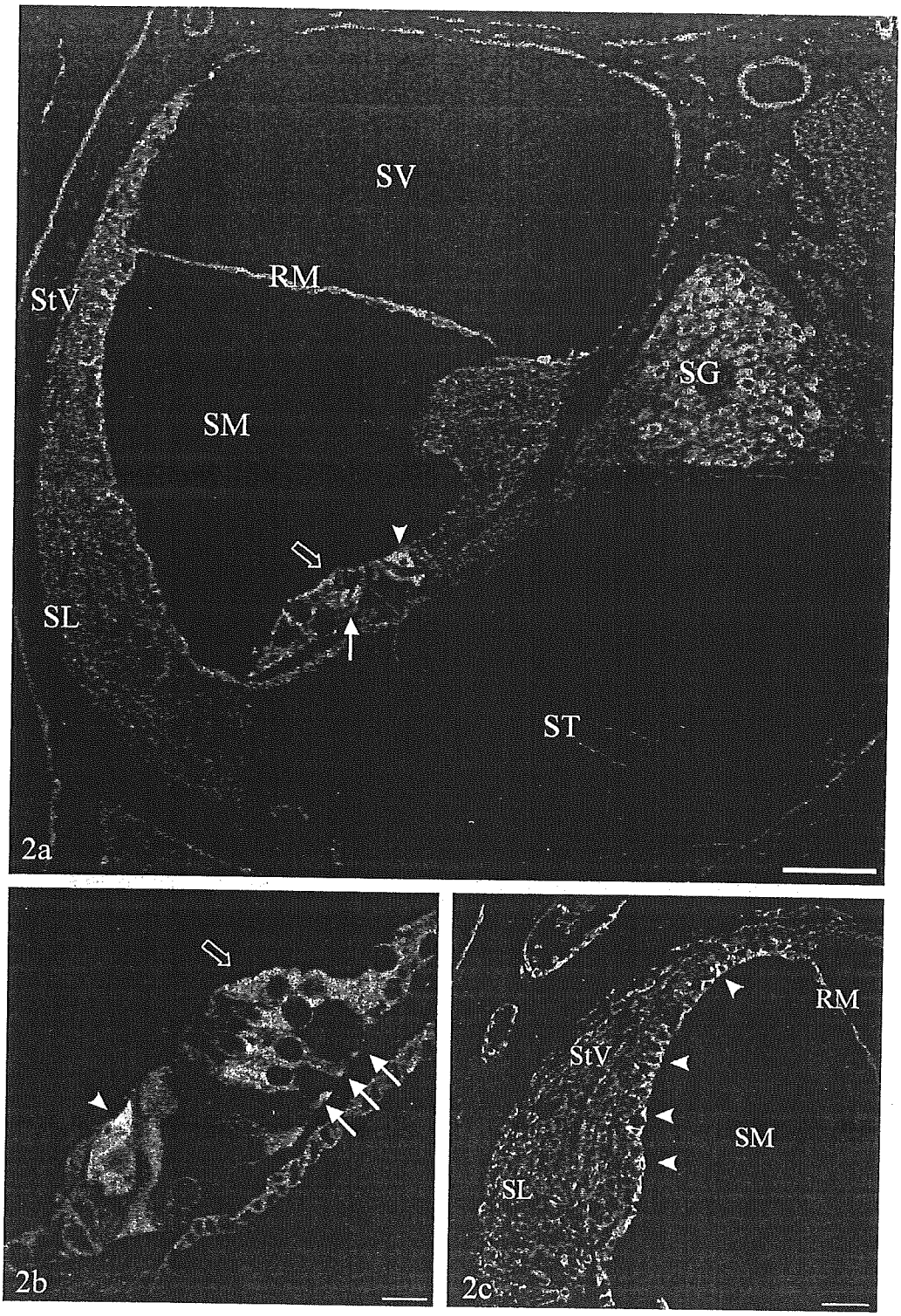

Fig. 2a–c Wolframin immunoreactivity in paraffin sections of PD14 mouse inner ear. *Scale bar* 50 μm. **a** Wolframin is strongly expressed in the spiral ganglion (*SG*), inner hair cell (*arrowhead*), Deiters' cells (*thin arrow*), and Hensen cells (*open arrow*). Moderate to strong reaction occurred in pillar cells, marginal cells of the stria vascularis (*StV*), and the Reissner's membrane (*RM*) and moderate to weak staining was observed in Claudius' cells, external sulcus cells, tympanic border cells, and outer hair cells. **b** Immunostaining in the organ of Corti was strong in the inner hair cell (*arrowhead*), Deiters' cells (*thin arrows*), and Hensen cells (*open arrow*). Moderate staining can be observed in pillar cells and tympanic border cells. Outer hair cells showed almost no immunoreactivity for wolframin. **c** Immunostaining of marginal cells (*arrowheads*) of the stria vascularis (*StV*), bordering the scala media (*SM*). No staining occurred in intermediate or basal cells of the stria vascularis. *SL* Spiral ligament, *ST* scala tympani, *SV* scala vestibuli

Strom et al. 1998), a 3.6-kb fragment was detected in several tissues. Band intensity was very strong in heart, strong in brain and kidney, moderate in lung and liver, weak in skeletal muscle and testis, and absent in spleen (data not shown). Digoxigenin-labeled sense and antisense mRNA probes were obtained and ISH was performed on PD1 mouse cochlear sections. Results with the antisense probe were consistent with the expression pattern observed by IHC (Fig. 6a, b), but in addition, ISH also showed expression in tympanic border cells, intermediate and basal cells of the stria vascularis, fibrocytes of the spiral ligament (Fig. 6b), and the supporting cells of the vestibular hair cells (data not shown). No significant signals were detected with the sense probe (Fig. 6c), when

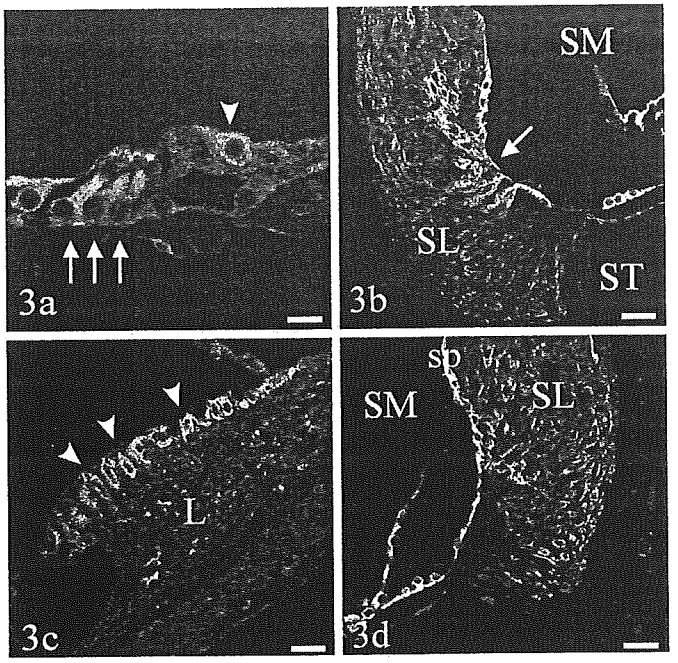

Fig. 3a–d Immunostaining for wolframin in paraffin sections of mature (PD35) mouse inner ear. *Scale bar* 50 μm. **a** In the organ of Corti, strong immunoreactivity was observed in the inner hair cell (*arrowhead*), Deiters' cells (*thin arrows*), and Hensen cells. No staining occurred in pillar cells or outer hair cells. **b** External sulcus cells (*thin arrow*) and their root processes showing strong wolframin expression. **c** Immunostaining in the interdental cells (*arrowheads*) of the spiral limbus. **d** Positive reaction in fibrocytes of the spiral ligament (*SL*). *L* Limbus, *SM* scala media, *sp* spiral prominence, *ST* scala tympani

the probe was omitted or when sections were RNase treated before hybridization.

Discussion

The *WFS1* gene, which encodes the wolframin protein, was identified as the causative gene for Wolfram syndrome or DIDMOAD by Inoue et al. and Strom et al. in 1998 (Inoue et al. 1998; Strom et al. 1998). The minimal diagnostic criteria for this autosomal recessive disease are diabetes mellitus and optic atrophy (Wolfram and Wagener 1938). Although diabetes insipidus and deafness are associated features, they are not invariably present. Interesting, heterozygous mutations in the same gene are responsible for low frequency HI in *DFNA6/14* patients (Bespalova et al. 2001; Young et al. 2001).

In this study, we analyzed expression of wolframin in mouse inner ear at different developmental stages to gain insight into its possible role in the biology of hearing. *WFS1* expression was observed in all developmental stages, suggesting that wolframin may be important (directly or indirectly) in auditory function. A differential expression pattern was noted at the different developmental stages, which may possibly be correlated to the physiological role of wolframin. Wolframin is strongly expressed at PD1, suggesting that it plays an important role during inner ear development. However, since wolframin expression persists at later stages, wolframin is probably also responsible for the maintenance of inner ear function. Next to its presence in inner ear, *WFS1* is ubiquitously expressed in other organs, an indication that wolframin is a common protein that is not exclusively associated with the hearing process.

Our results do indicate that expression of *WFS1* is concentrated in cells bordering the scala media, and in spiral ganglion and vestibular hair cells. Remarkably, *DFNA6/14* patients do not show symptoms of imbalance. In Wolfram syndrome patients, vestibular involvement has only been described in a limited number of cases and it is probably caused by central defects (Cremers et al. 1977; Higashi 1991; R.J. Pennings, personal communication). In *DFNA6/14* patients, normal vestibular function may be explained by the fact that these patients use visual and proprioceptive information to partly compensate the defect. However, this is less likely to be the case in patients with Wolfram syndrome as this is a progressive neurodegenerative disorder that includes polyneuropathy and optic atrophy. Wolframin may be less indispensable in the vestibular apparatus than in the cochlea.

Colocalization experiments with calreticulin, an ER-specific marker, indicated that wolframin is predominantly localized in this organelle, a finding consistent with data reported by Takeda et al. (2001). Noteworthy is the differential expression pattern of calreticulin in different cell types of the inner ear, and as a consequence, calreticulin is not an ideal marker for ER in all cell types of the inner ear. It shows strong immunoreaction in some cell types, while it is very weakly expressed in others. Notwithstanding this limitation, we noted a remarkable similarity between inner ear cells expressing wolframin and the presence of canalicular reticulum in these cells as described in the literature (for references, see Table 1). The canalicular reticulum is a specialized form of ER resembling the tubulocisternal ER which is present in some ion-transporting epithelia (Mollgard and Rostgaard 1978, 1981; Rostgaard and Moller 1980; Baron et al. 1984). The tubulocisternal reticulum and the canalicular reticulum are believed to facilitate transcellular movement of ions and fluid, an indispensable process in inner ear cells. The receptor potential of activated hair cells is generated by influx of K^+ from the endolymph. In order to prevent its cytotoxic accumulation in the hair cells and in order to maintain its concentration in the endolymphatic compartment, K^+ has to be recycled back to the endolymph. It has been suggested by Spicer and Schulte (1997) that the canalicular reticulum is important in this K^+ recycling pathway. Given the fact that wolframin is expressed in cells bordering the endolymphatic compartment and given the presence of canalicular reticulum in the same cell types, it is possible that *WFS1* plays a role in maintaining the ionic composition of the endolymph. Disruption of the *WFS1* gene may result in inadequate functioning of the canalicular reticulum and impaired K^+ recycling, leading to HI.

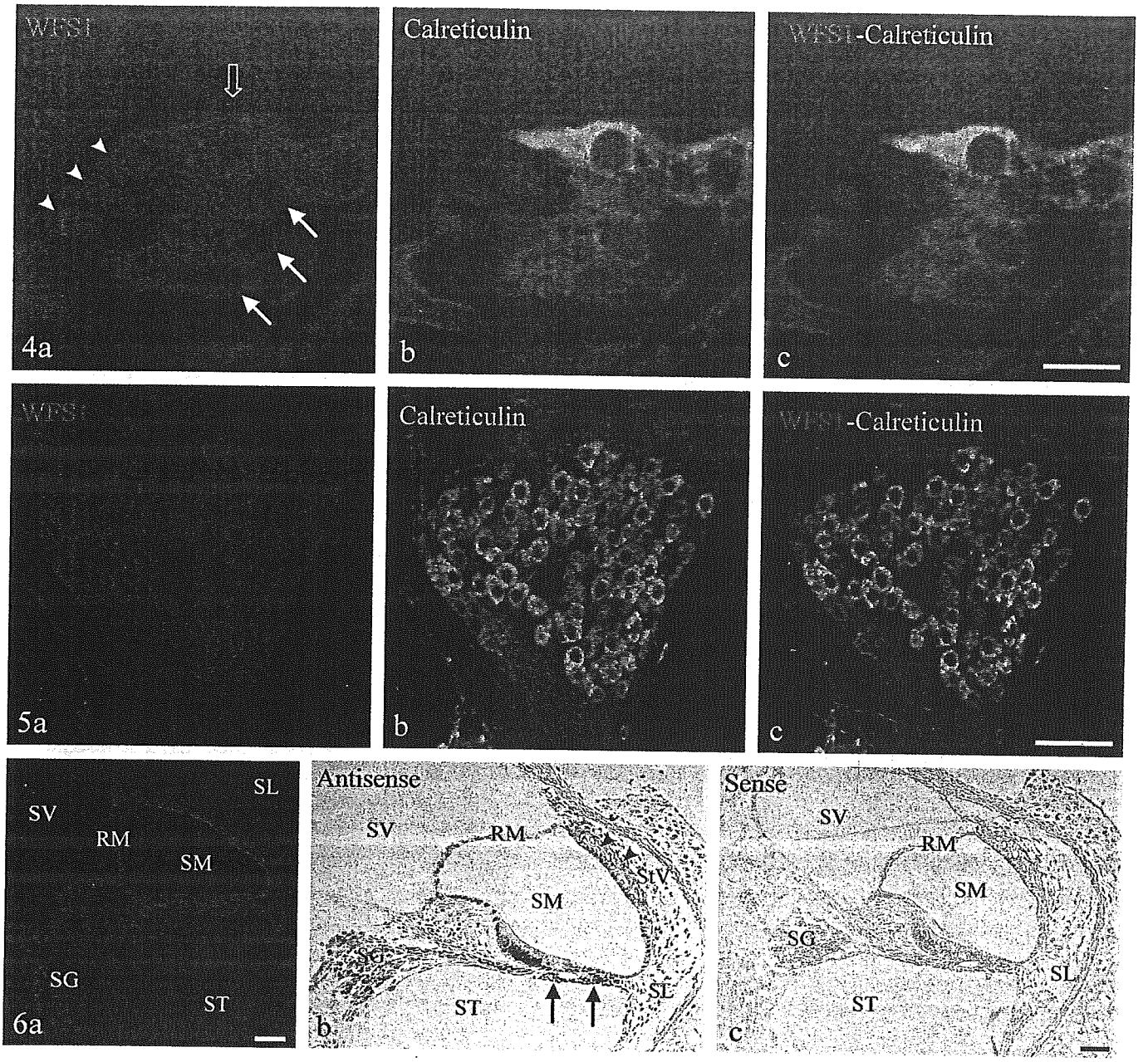

Fig. 4a–c Double labeling of wolframin and calreticulin in PD14 mouse inner ear showing colocalization of wolframin with the ER marker calreticulin. Detail of outer hair cells (*arrowheads*), Deiters' cells (*thin arrows*), and a Hensen cell (*open arrow*) in the organ of Corti. *Scale bar* 50 µm. **a** Strong wolframin expression is observed in Deiters' cells and a Hensen cell. Expression of wolframin in outer hair cells is very low. **b** Calreticulin expression. **c** Combined image of wolframin and calreticulin expression

Fig. 5a–c Double labeling of wolframin and calreticulin showing colocalization of wolframin with the ER marker calreticulin in the spiral ganglion of PD14 mouse cochlea. *Scale bar* 50 µm. **a** Wolframin immunolabeling. **b** Calreticulin immunolabeling. **c** Combined image of wolframin and calreticulin staining

Fig. 6 In situ hybridization (ISH) results (**b**, **c**) in comparison with results obtained by immunohistochemistry (IHC; **a**) for wolframin expression in PD1 mouse inner ear. *Scale bar* 50 µm. **a** Immunostaining of wolframin. **b** Staining pattern observed by ISH with digoxigenin (DIG)-labeled antisense mRNA probe (500 ng/ml) is consistent with the expression pattern observed by IHC (**a**), except for additional staining of tympanic border cells (*arrows*), intermediate and basal cells (*arrowheads*) of the stria vascularis (*StV*), and fibrocytes of the spiral ligament (*SL*). **c** ISH with DIG-labeled sense mRNA probe (500 ng/ml) showed no positive staining. *RM* Reissner's membrane, *SG* spiral ganglion, *SM* scala media, *ST* scala tympani, *SV* scala vestibuli

In the hearing process Ca^{2+} is also of functional importance. Mobilization of Ca^{2+} from an intracellular store (most likely the ER or its variant, the canalicular reticulum) occurs in spiral ganglion neurons (Rome et al. 1999), Deiters' cells (Dulon et al. 1994), vestibular hair cells (Lopez-Escamez and Schacht 1995), inner hair cells (Sugasawa et al. 1996b; Kennedy and Meech 2002), outer hair cells (Mammano et al. 1999), the non-sensory epithelial cells of the lateral cochlear wall (stria vascularis, spiral prominence, and external sulcus cells; Ikeda et al. 1995), Hensen cells (Sugasawa et al. 1996a), and pillar cells (Chung and Schacht 2002). We demonstrated the presence of wolframin in the ER of all these cell types, suggesting that this protein may be involved in the release and re-uptake of intracellular Ca^{2+} by the reticulum. Perhaps *WFS1* mutations disturb Ca^{2+} homeostasis, which could lead to cell death due to Ca^{2+} overload.

An important feature of the cochlea is that it is tonotopically organized in such a way that hair cells along the sensory epithelium respond best to acoustic stimulation at differing frequencies. As a consequence of this tonotopic organization, low frequencies are sensed at the cochlea's apex, while high frequencies are detected at its base. Our results revealed no gradient between apical and basal turns of the cochlea and on the basis of the expression pattern alone, we were not able to explain the differences in affected frequencies between *DFNA6/14* and Wolfram patients.

In conclusion, the expression pattern in murine inner ear suggests a possible role for wolframin in ion homeostasis (K^+ and/or Ca^{2+}) maintained by the canalicular reticulum. Although this hypothesis is difficult to test experimentally, the availability of a *WFS1* mouse model could offer an opportunity for further investigations. These studies are needed to determine the exact physiological role of wolframin in the biology of hearing and to gain more insight into its pathophysiological role in low frequency sensorineural HI and DIDMOAD.

Acknowledgements We thank Bradley Schulte for helpful discussion regarding the canalicular reticulum. K.C. holds a predoctoral position with the Institute for the Promotion of Innovation by Science and Technology in Flanders (IWT) and L.V.L. holds a research position with the Fund for Scientific Research Flanders (FWO). This study was supported by grant G.0277.01 from the FWO (G.V.C. and J.-P.T.) and grants from the University of Antwerp (G.V.C.) and NIDCD (RO1-DC03544, R.J.H.S.).

References

Baron DA, Briggman JV, Spicer SS (1984) Tubulocisternal endoplasmic reticulum in human eccrine sweat glands. Lab Invest 51:233–243

Bespalova IN, Camp G van, Bom SJ, Brown DJ, Cryns K, DeWan AT, Erson AE, Flothmann K, Kunst HPM, Kurnool P, Sivakumaran TA, Cremers CWRJ, Leal SM, Burmeister M, Lesperance MM (2001) Mutations in the Wolfram syndrome 1 gene (WFS1) are a common cause of low frequency sensorineural hearing loss. Hum Mol Genet 10:2501–2508

Chung JW, Schacht J (2002) ATP and nitric oxide modulate intracellular calcium in isolated pillar cells of the guinea pig cochlea. J Assoc Res Otolaryngol 2:399–407

Cremers CW, Wijdeveld PG, Pinckers AJ (1977) Juvenile diabetes mellitus, optic atrophy, hearing loss, diabetes insipidus, atonia of the urinary tract and bladder, and other abnormalities (Wolfram syndrome). A review of 88 cases from the literature with personal observations on 3 new patients. Acta Paediatr Scand Suppl 1–16

Cryns K, Pfister M, Pennings RJ, Bom SJ, Flothmann K, Caethoven G, Kremer H, Schatteman I, Koln KA, Toth T, Kupka S, Blin N, Nurnberg P, Thiele H, Heyning PH van de, Reardon W, Stephens D, Cremers CW, Smith RJ, Camp G van (2002) Mutations in the WFS1 gene that cause low-frequency sensorineural hearing loss are small non-inactivating mutations. Hum Genet 110:389–394

Cunningham CD, Weber PC, Spicer SS, Schulte BA (2000) Canalicular reticulum in vestibular hair cells. Hear Res 143:69–83

Dulon D, Blanchet C, Laffon E (1994) Photo-released intracellular Ca2+ evokes reversible mechanical responses in supporting cells of the guinea-pig organ of Corti. Biochem Biophys Res Commun 201:1263–1269

Forge A (1982) A tubulo-cisternal endoplasmic reticulum system in the potassium transporting marginal cells of the stria vascularis and effects of the ototoxic diuretic ethacrynic acid. Cell Tissue Res 226:375–387

Harada Y, Sakai T, Tagashira N, Suzuki M (1987) Three-dimensional observation of the cochlea. Intracellular structure of the hair cell and the supporting cell. Acta Otolaryngol 103:458–463

Higashi K (1991) Otologic findings of DIDMOAD syndrome. Am J Otol 12:57–60

Ikeda K, Suzuki M, Furukawa M, Takasaka T (1995) Calcium mobilization and entry induced by extracellular ATP in the non-sensory epithelial cell of the cochlear lateral wall. Cell Calcium 18:89–99

Inoue H, Tanizawa Y, Wasson J, Behn P, Kalidas K, Bernal-Mizrachi E, Mueckler M, Marshall H, Donis-Keller H, Crock P, Rogers D, Mikuni M, Kumashiro H, Higashi K, Sobue G, Oka Y, Permutt MA (1998) A gene encoding a transmembrane protein is mutated in patients with diabetes mellitus and optic atrophy (Wolfram syndrome). Nat Genet 20:143–148

Kennedy HJ, Meech RW (2002) Fast Ca2+ signals at mouse inner hair cell synapse: a role for Ca2+-induced Ca2+ release. J Physiol 539:15–23

Lopez-Escamez JA, Schacht J (1995) Mechanically induced calcium increases in isolated vestibular hair cells of the guinea pig. Acta Otolaryngol 115:759–764

Lynch ED, Lee MK, Morrow JE, Welcsh PL, Leon PE, King MC (1997) Nonsyndromic deafness DFNA1 associated with mutation of a human homolog of the Drosophila gene diaphanous. Science 278:1315–1318

Mammano F, Frolenkov GI, Lagostena L, Belyantseva IA, Kurc M, Dodane V, Colavita A, Kachar B (1999) ATP-Induced Ca(2+) release in cochlear outer hair cells: localization of an inositol triphosphate-gated Ca(2+) store to the base of the sensory hair bundle. J Neurosci 19:6918–6929

Michalak M, Milner RE, Burns K, Opas M (1992) Calreticulin. Biochem J 285:681–692

Mollgard K, Rostgaard J (1978) Morphological aspects of some sodium transporting epithelia suggesting a transcellular pathway via elements of endoplasmic reticulum. J Membr Biol 40(Spec No):71–89

Mollgard K, Rostgaard J (1981) The transcellular compartment of tubulocisternal endoplasmic reticulum, a common feature of transporting epithelial cells. In: Ussing HH, Bindslev N, Sten-Knudsen O (eds) Water transport across epithelia. Munksgaard, Copenhagen, pp 85–98

Nash PD, Opas M, Michalak M (1994) Calreticulin: not just another calcium-binding protein. Mol Cell Biochem 135:71–78

Qvortrup K, Rostgaard J (1990) Three-dimensional organization of a transcellular tubulocisternal endoplasmic reticulum in epithelial cells of Reissner's membrane in the guinea-pig. Cell Tissue Res 261:287–299

Rome C, Luo D, Dulon D (1999) Muscarinic receptor-mediated calcium signaling in spiral ganglion neurons of the mammalian cochlea. Brain Res 846:196–203

Rostgaard J, Moller O (1980) Localization of Na+, K+-ATPase to the inside of the basolateral cell membranes of epithelial cells of proximal and distal tubules in rabbit kidney. Cell Tissue Res 212:17–28

Spicer SS, Schulte BA (1997) Golgi–canalicular reticulum system in ion transporting fibrocytes and outer sulcus epithelium of gerbil cochlea. Anat Rec 249:117–127

Spicer SS, Thomopoulos GN, Schulte BA (1998) Cytologic evidence for mechanisms of K+ transport and genesis of Hensen bodies and subsurface cisternae in outer hair cells. Anat Rec 251:97–113

Spicer SS, Thomopoulos GN, Schulte BA (1999) Novel membranous structures in apical and basal compartments of inner hair cells. J Comp Neurol 409:424–437

Spicer SS, Thomopoulos GN, Schulte BA (2000) Structural evidence for ion transport and tectorial membrane maintenance in the gerbil limbus. Hear Res 143:147–161

Strom TM, Hortnagel K, Hofmann S, Gekeler F, Scharfe C, Rabl W, Gerbitz KD, Meitinger T (1998) Diabetes insipidus, diabetes mellitus, optic atrophy and deafness (DIDMOAD) caused by mutations in a novel gene (wolframin) coding for a predicted transmembrane protein. Hum Mol Genet 7:2021–2028

Sugasawa M, Erostegui C, Blanchet C, Dulon D (1996a) ATP activates a cation conductance and Ca(2+)-dependent Cl-conductance in Hensen cells of guinea pig cochlea. Am J Physiol 271:C1817–C1827

Sugasawa M, Erostegui C, Blanchet C, Dulon D (1996b) ATP activates non-selective cation channels and calcium release in inner hair cells of the guinea pig cochlea. J Physiol 491:707–718

Takeda K, Inoue H, Tanizawa Y, Matsuzaki Y, Oba J, Watanabe Y, Shinoda K, Oka Y (2001) WFS1 (Wolfram syndrome 1) gene product: predominant subcellular localization to endoplasmic reticulum in cultured cells and neuronal expression in rat brain. Hum Mol Genet 10:477–484

Van Camp G, Smith RJH (2002) Hereditary hearing loss homepage. http://dnalab-www.uia.ac.be/dnalab/hhh. Cited October 2002

Wolfram DJ, Wagener HP (1938) Diabetes mellitus and simple optic atrophy among siblings: report of four cases. Mayo Clin Proc 13:715–718

Young TL, Ives E, Lynch E, Person R, Snook S, MacLaren L, Cator T, Griffin A, Fernandez B, Lee MK, King MC (2001) Non-syndromic progressive hearing loss DFNA38 is caused by heterozygous missense mutation in the Wolfram syndrome gene WFS1. Hum Mol Genet 10:2509–2514

OBSERVATIONS

Multiple Cranial Mononeuropathies With Acetylcholine Receptor Antibody in Mitochondrial Diabetes

In 1997, we reported the first identified case of mitochondrial diabetes caused by a T-to-C transition at position 3264 (1). The patient had type 2 diabetes, lipoma, facial palsy, ophthalmoplegia, and hearing loss. His unique profile suggests the heterogeneity of mitochondrial (mt)DNA-related diabetes. Among the characteristics, bilateral facial palsy and ophthalmoplegia (right eye) were noteworthy because they have not been reported in mitochondrial diabetes associated with other pathogenetic mutations. At age 59 years, facial palsy appeared first on the right side and 6 months later on the left side. It occurred without pain and became persistent. At age 64, ophthalmoplegia occurred with transient ocular pain with ptosis and pupillary sparing. Interestingly, during the follow-up we observed that serum acetylcholine receptor antibody was positive at age 65 years (0.6 nmol/l; the titer is considered to be positive at >0.2 nmol/l, which is 2 SD above the mean of 170 normal control subjects). Edrophonium chloride (Tensilon) test was negative. Repetitive nerve stimulation was negative, and GAD antibody was negative.

Disordered autoimmunity such as islet cell antibody (ICA) and GAD antibody has been described in several case reports of mitochondrial diabetes or MELAS (mitochondrial encephalopathy, lactic acidosis, and stroke-like episodes) (2–4). As for acetylcholine receptor antibody, it has been reported in two elderly women with external ophthalmoplegia; one of the two women had diabetes (5). Because ragged-red fibers and elevated lactic acid were observed in the patients, Mitsikostas et al. pointed out that ophthalmoplegia and acetylcholine receptor antibody are correlated with mitochondrial myopathies. Therefore, in this case, the association of cranial nerve palsies and positive acetylcholine receptor antibody may not be a fortuitous coincidence. It was speculated that mitochondrial DNA abnormality causes not only diabetes but also the immune destruction associated with acetylcholine receptor antibody, which develops bilateral facial nerve palsy and ophthalmoplegia.

However, as for ophthalmoplegia, this patient's condition was complicated with ocular pain at onset and did not respond to the tensilon test. Because pain is not a manifestation of myasthenia gravis, vascular factors may be involved, overlapping on the pathogenesis of autoimmune factor. Since the report of Asbury et al. (6) in 1970, the etiology to understand ophthalmoplegia in diabetes has been hypothesized to result from diabetic microvascular injury involving small vessels that supply nerves. This patient had strongly succinate dehydrogenase reactive vessels that contained proliferation of abnormal mitochondria in the smooth muscle cells (1). Therefore, the ophthalmoplegia might be triggered by vascular events associated with a proliferation of abnormal mitochondria in vascular smooth muscle cells. Thus, this case suggests that cranial mononeuropathies in diabetes could possibly be caused by the synergistic effects of mitochondrial genetic abnormality, disordered autoimmunity, and/or microvascular abnormality.

YOSHIHIKO SUZUKI, MD[1,2,3]
S. SUZUKI, MD[4]
M. TANIYAMA, MD[2]
T. MURAMATSU, MD[5]
S. OHTA, PHD[3]
Y. OKA, MD[4]
Y. ATSUMI, MD[1]
K. MATSUOKA, MD[1]

From [1]Saiseikai Central Hospital, Tokyo, Japan; [2]Fujigaoka Hospital, Showa University, Kanagawa, Japan; the [3]Department of Biochemistry and Cell Biology, Institute of Gerontology, Nippon Medical School, Kanagawa, Japan; the [4]Division of Molecular Metabolism and Diabetes, Department of Internal Medicine, Tohoku University Graduate School of Medicine, Miyagi, Japan; and the [5]Department of Neuropsychiatry, Keio University, Tokyo, Japan

Address correspondence and reprint requests to Yoshihiko Suzuki, MD, Saiseikai Central Hospital, 1-4-17, Mita, Minato-ku, Tokyo, 108 Japan. E-mail: drsuzuki@cts.ne.jp.

Acknowledgments— The authors thank Professor S. Yagihashi for giving advice and reviewing the manuscript.

References

1. Suzuki Y, Suzuki S, Hinokio Y, Chiba M, Atsumi Y, Hosokawa K, A Shimada A, Asahina T, Matsuoka K: Diabetes associated with a novel 3264 Mitochondrial $tRNA^{Leu(UUR)}$ mutation. *Diabetes Care* 20: 1138–1140, 1997
2. Oka Y, Katagiri H, Yazaki Y, Murase T, Kobayashi T: Mitochondrial gene mutation in islet-cell-antibody-positive patients who were initially non-insulin-dependent diabetics. *Lancet* 342:527–528, 1993
3. Suzuki Y, Taniyama M, Shimada A, Atsumi Y, Matsuoka K, Oka Y: GAD antibody in mitochondrial diabetes associated with $tRNA^{(UUR)}$ mutation at position 3271 (Letter). *Diabetes Care* 25:1097–1098, 2002
4. Ohno K, Yamamoto M, Engel AG, Harper CM, Roberts LR, Tan GH, Fatourechi V: MELAS- and Kearns-Sayre-type: co-mutation with myopathy and autoimmune polyendocrinopathy. *Ann Neurol* 40:480, 1996
5. Mitsikostas D, Manta P, Kalfakis N, Chioni A, Ilias A, Liakopoulos D, Papageorgiou C: External ophthalmoplegia with ragged-red fibers and acetylcholine receptor antibodies. *Funct Neurol* 10: 209–215, 1995
6. Asbury AK, Aldredge H, Hershberg R, Fisher CM: Occulomotor palsy in diabetes mellitus: a clinicopathological study. *Brain* 93:555, 1970

AQ: A

ELSEVIER

Mitochondrion 2 (2003) 293–304

Mitochondrion

www.elsevier.com/locate/mito

A novel mtDNA C11777A mutation in Leigh syndrome

Hirofumi Komaki[a], Jun Akanuma[a], Hideki Iwata[b], Takao Takahashi[c], Yukihiko Mashima[d], Ikuya Nonaka[e], Yu-ichi Goto[a,*]

[a]*Department of Mental Retardation and Birth Defect Research, National Institute of Neuroscience, National Center of Neurology and Psychiatry (NCNP), 4-1-1 Ogawahigashi, Kodaira, Tokyo 187-8502, Japan*

[b]*Department of Pediatrics, Shinshiro City Hospital, 32-1 Kitahata, Shinshiro, Aichi 441-1387, Japan*

[c]*Department of Pediatrics, School of Medicine, Keio University, 35 Shinanomachi, Shinjuku, Tokyo 160-8582, Japan*

[d]*Department of Opthalmology, School of Medicine, Keio University, 35 Shinanomachi, Shinjuku, Tokyo 160-8582, Japan*

[e]*National Center Hospital for Mental, Nervous and Muscular Disorders, National Center of Neurology and Psychiatry (NCNP), 4-1-1 Ogawahigashi, Kodaira, Tokyo 187-8551, Japan*

Received 27 August 2002; received in revised form 4 December 2002; accepted 17 December 2002

Abstract

A novel mitochondrial DNA point mutation, a C-to-A mutation at nucleotide position (np) 11,777, was identified in two unrelated patients out of 100 with Leigh syndrome. This mutation converted a highly evolutionary conserved arginine to a serine at codon 340 in ND4 gene. This codon was also converted by a G-to-A mutation at np 11,778, the most common mutation associated with Leber's hereditary optic neuropathy (LHON), but the amino acid replacement was different (R340S vs. R340H). Cybrid study revealed that the percentage of heteroplasmy was correlated with complex I function and that the novel mutation caused a much more deleterious effect than the np 11,778 LHON mutation in complex I activity.

Keywords: Mitochondrial disease; Complex I deficiency; Heteroplasmy; Cybrid; ATP production

1. Introduction

Leigh syndrome (LS) is a subacute neurodegenerative disease of infancy and childhood characterized by symmetrical necrotic lesions in the brainstem, basal ganglia and thalamus (Leigh, 1951). The symptoms include psychomotor retardation or deterioration, failure to thrive, vomiting, seizures and respiratory failure. Elevated lactate levels in blood and spinal fluid are consistent laboratory findings. With recent technological advances, especially in neuroimaging techniques, many patients are being diagnosed with LS while still alive. LS is a mitochondrial but heterogeneous disease. Biochemically, defects in the pyruvate dehydrogenase complex and respiratory chain complexes including complexes I, II, IV and V have been documented. Genetically, defects in both mitochondrial DNA (mtDNA) and nuclear DNA are reportedly involved in the pathogenesis of LS. The defects in mtDNA include T-to-G (Tatuch et al., 1992) and T-to-C (de Vries et al., 1993) at nucleotide position (np) 8993 and T-to-C (Thyagarajan et al., 1995) and T-to-G (Carrozzo et al., 2001) at np 9176 in the subunit 6 gene of adenine-trinucleotide phosphate (ATP) synthase, A-to-G at np

* Corresponding author. Tel.: +81-42-346-1713; fax: +81-42-346-1743.

E-mail address: goto@ncnp.go.jp (Y. Goto).

1567-7249/03/$20.00
doi:10.1016/S1567-7249(03)00003-5

3243 (Sue et al., 1999), and A-to-G at np 8344 (Silvestri et al., 1993) in the mitochondrial transfer RNA gene, and G-to-A at np 14,459 in the subunit 6 gene of complex I (Kirby et al., 2000). The defects in nuclear DNA include the E1 alpha subunit gene of pyruvate dehydrogenase complex (Endo et al., 1989), the NDUFS4 (van den Heuvel et al., 1998), NDUF7 (Triepels et al., 1999), NDUFS8 (Loeffen et al., 1998), and NDUFS1 (Benit et al., 2001) genes of complex I, the flavoprotein subunit gene of complex II (Bourgeron et al., 1995), and the SURF (Surfeit locus protein)-1 gene, an assembly factor for cytochrome-*c*-oxidase (COX) (Zhu et al., 1998). Nevertheless, in more than half of LS patients, the pathogenesis cannot be identified.

Complex I is a large multiprotein assembly, which is partly located in the mitochondrial inner membrane and partly protrudes into the matrix. Its main function is transport of electrons from NADH to ubiquinone with simultaneous shunting of protons across the inner mitochondrial membrane to the intermembrane space (Loeffen et al., 2000). Complex I is composed of at least 42 distinct subunits. Seven subunits of human complex I are encoded by mtDNA (DiMauro et al., 1999). Defects of complex I are a major cause of mitochondrial disease, and many pathogenic mutations in the subunits of complex I and transfer RNA of mtDNA and nuclear encoded subunits of complex I have been reported (Shoubridge, 2001).

We herein report a novel mtDNA mutation associated with LS with isolated complex I deficiency in two unrelated patients. This is a C-to-A mutation at np 11,777, which converts a highly evolutionary conserved arginine to a serine at codon 340 in the NADH dehydrogenase subunit 4 (ND4) gene in mtDNA. Interestingly, this codon is also converted by G-to-A mutation at np 11,778, the most common mutation associated with Leber's hereditary optic neuropathy (LHON) (Wallace et al., 1988).

2. Materials and methods

2.1. Subjects

Patient 1 was a 4-year-old girl, the second child of healthy and unrelated Japanese parents. Her family history was negative for neurological disease and diabetes. She was born at term in a normal delivery. Her development was mildly retarded. She could hold her head steady at 3 months, sit up at 7 months, walk by herself at 20 months and speak meaningful words at 24 months of age. Clinical examination at 3 years and 5 months of age revealed a short stature (less than 3rd percentile), but no minor anomalies nor arrhythmia. She had exotropia in the right eye, but no abnormalities in ocular movement or eyeground by the fundoscopic examination. She could walk and run without support and speak meaningful words, but she could not speak sentences. Her deep tendon reflexes and muscle power were normal, but muscle tone and bulk were mildly reduced. She had no involuntary movements, cerebellar signs, or autonomic disturbances. She had no signs of psychomotor deterioration. Laboratory examination revealed relatively high lactate compared to pyruvate in both blood (lactate 45.5 mg/dl, pyruvate 1.2 mg/dl; normal 6.5–18.3, 0.71–1.22, respectively) and spinal fluid (lactate 31.5, pyruvate 1.68; normal 11.1–16.3, 0.75–1.29, respectively) which is consistent with respiratory chain defect. Brain magnetic resonance imaging (MRI) showed abnormal high T2-weighted signals in the bilateral midbrain and thalamus.

Patient 2 was a 5-year-old girl, the first and only child of healthy and unrelated parents. She was born at term in a normal delivery. Her family history was negative for neurological disease and diabetes. Her development was mildly retarded. She showed deterioration and dystonia from 3 years old. Clinical examination at 4 years of age showed her to be of short stature (less than three percentile), but revealed no minor anomalies, or arrhythmia. She had exotropia and a disturbance of adduction in her left eye, but no abnormalities in the eyegrounds by fundoscopic examination. Her deep tendon reflexes were hyperactive. Muscle power, tone and bulk were normal. She had dystonia in the upper and lower extremities. Laboratory examination revealed normal to slightly elevated lactate and pyruvate levels in blood (lactate 10.1–19.1 mg/dl, pyruvate 0.51–1.25 mg/dl; normal 6.5–18.3, 0.71–1.22, respectively), and moderately elevated levels in the spinal fluid (lactate 31.7 mg/dl, pyruvate 1.39 mg/dl; normal 11.1–16.3, 0.75–1.29, respectively). Brain and spinal cord MRI revealed

abnormal high T2-weighted signals in the bilateral basal ganglia, substantia nigra and cervical cord.

2.2. Histopathological studies

For histochemical examination, muscle specimens were frozen in isopentane chilled in liquid nitrogen. Serial frozen sections, 10 μm in thickness, were stained with hematoxylin–eosin, modified Gomori trichrome (mGT), NADH-tetrazolium reductase (NADH-TR), succinate dehydrogenase (SDH), COX, and a battery of histochemical methods.

2.3. Cell culture

Primary muscle cultures were obtained from muscle biopsies. Fibroblast culture was available only in patient 1. To eliminate fibroblast contamination, we used the preplating technique for the preparation of myoblasts (Miranda, 1994; Richler and Yaffee, 1970). Myoblasts and fibroblasts were grown in DMEM/F-12 medium with 20% fetal bovine serum (GIBCO-BRL).

2.4. Direct sequence of total mtDNA

DNA extraction, PCR and total mtDNA sequencing were done as described elsewhere (Akanuma et al., 2000). The nuclear DNA carries sequences similar to those of the mtDNA (nuclear pseudogene), and it has several point mutations previously reported to be pathogenic. To minimize the adverse effect of the nuclear pseudogene, we employed the long PCR method in preparing the template of the sequencing reaction.

2.5. Restriction fragment length polymorphism (RFLP) analysis of mtDNA mutations

The following sets of primers were used for the detection of the C-to-A mutation at np 11,777. A light-strand primer, corresponding to np 11,666–11,685, and a modified heavy-strand primer, corresponding to np 11,798–11,778 (5′-CTTGAGAGAG-GATTATGAAGC-3′), were used. The underlined position represented a modification from the normal sequence to create an Alu I restriction site (AGCT) when the mutant sequences were amplified. The amplified 133 base pair fragment was digested with Alu I to produce 112 + 21 base pairs for the wild type sequence, and 93 + 21 + 19 base pairs for the mutant sequence. These fragments were separated electrophoretically through a 4.0% low melting agarose gel after ethidium bromide staining.

2.6. Quantification of the np 11,777 mutation using real-time polymerase chain reaction (PCR) amplification methods

The target sequence of the mtDNA was amplified using a light-strand primer, corresponding to np 11,730–11,757 and a heavy-strand primer, corresponding to np 11,845–11,817, was used to amplify the target sequence in the presence of two fluorogenic TaqMan™ probes. One was a FAM-labeled probe for the detection of the wild type sequence [5′(FAM)-CTCACAGTCGCATCAT-(MGB: minor groove binder)p3′], and the other was a VIC-labeled probe for the mutant type sequence [5′(VIC)-CTCACAG-TAGCATCAT-(MGB)p3′]. The underlined position corresponded to np 11,777. The PCR condition was 2 min at 50°C, 10 min at 95°C, 40 cycles with 15 s at 95°C, and 1 min at 60°C. During the PCR, the respective TaqMan™ probe hybridized to the wild type or the mutant template and Taq DNA polymerase synthesizes a new strand and cleaves off each reporter dye simultaneously, increasing the intensity of the fluorescence signal which corresponds to the initial amount of template mtDNA. The level of fluorescence was simultaneously monitored on an ABI PRISM 7700 Sequence Detector System (PE Applied Biosystem) to determine the threshold cycle (CT), at which the fluorescence exceeds the baseline. The copy number of mtDNA containing each mutant or wild type sequence was determined based on the standard curve created by the reaction of the known amount of plasmid containing mtDNA fragment (np 10,660–12,665) with each wild or mutant sequence made by standard PCR following TA-cloning technique. All PCR assays were carried out in triplicate, and the proportion of the mutation was calculated by the following equation: the copy number of mutant type myDNA × 100/ (the copy number of wild type mtDNA + the copy number of mutant type mtDNA).